

Spatial variations of hot-carrier transmission across CoSi₂/Si interfaces on a nanometer scale

H. Sirringhaus, T. Meyer, E. Y. Lee, and H. von Känel

Laboratorium für Festkörperphysik, Eidgenössische Technische Hochschule, Zürich, CH-8093 Zürich

(Received 22 November 1995)

In situ ballistic-electron-emission microscopy (BEEM) and spectroscopy have been performed at 77 K on epitaxial CoSi₂ films on *n*-Si(100) and Si(111) of both doping types. Two different mechanisms have been identified, by which structural defects at these interfaces give rise to variations of the carrier transmission across the interface on a nanometer scale: On CoSi₂/Si(111) interfacial misfit dislocations locally enhance the scattering probability at the interface. By the same mechanism individual interfacial point defects can be resolved in BEEM images. No variations of the Schottky barrier have been observed at this interface. In contrast, on CoSi₂/Si(100), certain interfacial dislocations and other defects lower the Schottky barrier by up to 0.1 eV on a nanometer scale. [S0163-1829(96)05124-7]

I. INTRODUCTION

The trend in modern microelectronic technology to reduce device dimensions is still unbroken. At present typical feature sizes in a very large scale integration circuit are on the order of 0.5 μm . Recently, the operation of a metal-oxide-semiconductor field effect transistor with a gate length of only 40 nm has been demonstrated.¹ The performance of such an ultrasmall device will be increasingly influenced by local fluctuations of the material properties on a nanometer scale, rather than their average over μm dimensions. In particular, inhomogeneities of the semiconductor heterointerfaces, such as individual local charges, nanometer-scale interfacial disorder, point and line defects, etc. will affect the device characteristics. Therefore, there arises the need to investigate carrier transport across interfaces on a truly *microscopic* scale.

This has become possible with the invention of ballistic-electron-emission microscopy (BEEM) and spectroscopy (BEES) by Kaiser and Bell.² BEEM is an extension of a two-terminal (tip-sample) scanning tunneling microscopy (STM) experiment to a transistorlike configuration. The STM tip is used to inject hot carriers into a metallic base layer on top of a semiconductor heterostructure. By measuring the fraction I_c of the total tunneling current I_t , which is finally collected in the semiconducting substrate, one can extend the spatial resolution capabilities of STM to the study of the transport across the buried interfaces. BEEM has mainly been applied to simple metal-semiconductor (*M-S*) contacts,³ but also to more complicated structures such as *p-n* diodes,⁴ semiconductor heterojunctions,⁵ resonant tunneling structures,⁶ metal-insulator-semiconductor,⁷ metal-oxide-semiconductor⁸ structures.

The purpose of the present work is to investigate the mechanisms, by which individual interfacial defects affect the hot-carrier transmission across a simple, epitaxial *M-S* interface. To resolve spatial variations of the carrier transmission around individual interfacial defects the spatial resolution capabilities of the BEEM technique have to be fully exploited. This has become possible by (a) performing the experiment *in situ* and at low temperatures (77 K), and (b) choosing a well-ordered epitaxial base layer (CoSi₂ on Si) with atomically smooth surfaces and interfaces. In this way scattering of the carriers in the metal and at its surface is

reduced. Scattering in the base broadens the electron beam injected by the STM tip, i.e., deteriorates the spatial resolution of interfacial inhomogeneities, and also renders the interpretation of BEEM images more complicated. CoSi₂/Si is one of the prototype systems of the epitaxial *M-S* interface.

Individual interfacial defects have been found to give rise to contrast in BEEM images by two different mechanisms.

(1) Interfacial defects perturb the lattice periodicity in the interface plane and, therefore, scatter the carriers incident upon the interface. In a previous study⁹ we have reported on the observation of scattering at interfacial *misfit dislocations* at the CoSi₂/Si(111) interface. Here, we focus on scattering at individual interfacial *point defects* at this interface. Point defects have been resolved in BEEM images with a density of 10^{12} – 10^{13} cm^{-2} . This establishes BEEM as one of the few experimental techniques, by which individual interfacial point defects can be detected. Their observation, which has become possible by a further improvement of the signal-to-noise ratio compared to our earlier experiments, enables us to take BEES spectra in perfectly ordered interfacial regions, i.e., regions that contain neither dislocations nor point defects. These spectra give new insight into carrier scattering mechanisms at this epitaxial interface as well as into the still puzzling absence of a delayed BEES onset in the experimental CoSi₂/Si(111) BEES spectra. Such a delayed onset is predicted by theory¹⁰ (Sec. III).

(2) Apart from scattering, dislocations may also give rise to a change of the band lineup at the interface, because the local atomic interface structure can affect the interface dipole and the height of the Schottky barrier Φ_b . At the CoSi₂/Si(100) interface a lowering of Φ_b around certain dislocations and other defects has been observed. In contrast, such spatial variations of Φ_b do not occur at the CoSi₂/Si(111) interface. The role of interfacial defects in pinning the Fermi level at a *M-S* interface has been pointed out by Spicer *et al.*,¹¹ but is still not understood completely,¹² although being of crucial practical and fundamental importance (Sec. IV).

II. EXPERIMENT

CoSi₂ films have been grown by molecular beam epitaxy (MBE) on *n*-Si(100) and Si(111) of both doping types. All films are single crystalline with the (100) and (111) planes,

respectively, of the silicide parallel to the Si substrate. The films do not contain any grain boundaries. The substrates are degenerately doped 3-in. Si wafers ($n^+, p^+ > 10^{19} \text{ cm}^{-3}$). Before deposition of the silicide a 3000-Å undoped Si buffer layer is grown. The residual doping in the buffer layer has been measured to be below 10^{15} cm^{-3} . Details about the growth procedure can be found in Refs. 13 and 14.

The STM and BEEM experiments have been performed at 77 K in a home-built, low-temperature UHV STM suited for 3-in. wafers.¹⁵ Chemically etched tungsten tips have been cleaned by Ar sputtering in the STM chamber. All BEES spectra have been taken in the constant current mode, and have been normalized to a tunneling current $I_t = 1 \text{ nA}$. The value of I_t , with which the spectra have been taken, is indicated in the figure captions.

III. HOT-CARRIER SCATTERING AT POINT DEFECTS AND DISLOCATIONS AT THE $\text{CoSi}_2/\text{Si}(111)$ INTERFACE

In a previous work it has been shown that individual misfit dislocations at the $\text{CoSi}_2/\text{Si}(111)$ interface can be resolved by BEEM. They give rise to a sharply localized increase of the BEEM current on $\text{CoSi}_2/n\text{-Si}(111)$ (see dashed line in Fig. 1) (Ref. 9) and a decrease on $\text{CoSi}_2/p\text{-Si}(111)$.¹⁶ At the dislocations we do *not* observe a variation of the Schottky barrier. In the case of $n\text{-Si}$, spectra taken on top of a dislocation set in at $0.66 \pm 0.03 \text{ eV}$, at the same value as those in the neighboring dislocation free regions [see Fig. 2(a)]. The contrast at the dislocations is rather due to carrier scattering at the dislocation core, which perturbs the lattice periodicity in the interface plane. The interface transmission probability (ITP) $T(E, k_{\parallel})$ close to the BEES threshold is nonzero only for electrons with a sufficiently large momentum component k_{\parallel} in the $\text{CoSi}_2/n\text{-Si}(111)$ interface Brillouin zone (IBZ). This is so because the Si conduction-band minima (CBM) close to the X point project onto a point $k_{\parallel}^0 = 0.8 \text{ \AA}^{-1}$ away from the zone center of the (111) IBZ. In contrast, on $\text{CoSi}_2/p\text{-Si}(111)$, holes are transmitted into the zone centered valence-band maximum. The angular distribution of the carriers injected by the STM tip is forward focused, i.e., mainly contains electrons with $k_{\parallel} \approx 0$. Therefore, interface scattering providing the carriers with an additional k_{\parallel} component is expected to increase the BEEM current in the case of $\text{CoSi}_2/n\text{-Si}(111)$ and to decrease it on $\text{CoSi}_2/p\text{-Si}(111)$, as observed in the experiment.^{9,16}

Here, we focus on the observation of individual interfacial point defects by the same contrast mechanism. Figure 1 displays a STM topograph (a) and BEEM image (b) of a 32-Å $\text{CoSi}_2/n\text{-Si}(111)$ film. Apart from the contrast at dislocations (see dashed line) we also observe an increase of the BEEM current by $\approx 10\%$ in pointlike regions (A). By taking STM topographs at low tip voltage ($V_t \leq 0.1 \text{ V}$), where the unreconstructed atomic surface structure of the silicide can be resolved, it has been verified that the current enhancement in region (A) cannot be attributed to surface point defects. The surface in region (A) is perfectly ordered. Therefore, the contrast has to be attributed to subsurface point defects, located either in the silicide or at the buried interface. We regard the second possibility as being more likely because the average distance between those point defects is on the order of 50–

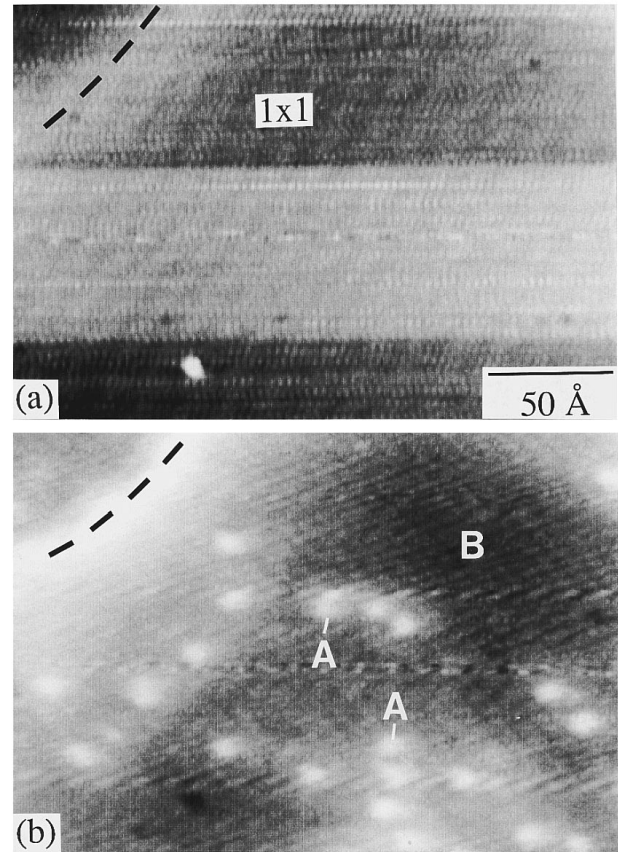


FIG. 1. STM topograph (a) and BEEM image (b) of a 32-Å $\text{CoSi}_2/n\text{-Si}(111)$ film. The corrugation in the STM topography image is not due to the unreconstructed (1×1) atomic surface structure but due to a small mechanical vibration. The BEEM current is enhanced at individual interfacial dislocations (dashed line) and subsurface point defects (A) due to hot carrier scattering. ($V_t = -1.8 \text{ V}$, $I_t = 10 \text{ nA}$).

100 Å, whereas for bulk CoSi_2 as well as for thick CoSi_2 films mean free path lengths λ of the order of 1000 Å (at 4.2 K) have been measured for electron energies close to E_F .¹⁷ Only when the film thickness is below 50 Å does the residual resistivity increase, giving evidence for nonspecular scattering either at the surface or the interface.¹⁸

The spatial resolution of the point defects is determined by the spatial extent of the injected electron beam at the interface, rather than the physical size of the point defects themselves. This we conclude from the observation that the full width at half maximum (FWHM) of the BEEM profiles across a point defect depends significantly on the tip conditions. On thin films ($d \approx 20\text{--}30 \text{ \AA}$) the FWHM is smaller for sharp than for blunt tips. The sharpness of the tip is estimated from the STM topography resolution.¹⁹ A typical value for the FWHM is 1 nm. Therefore, the physical size of the point defects must be smaller than 1 nm; i.e., it must be on the atomic scale. Although from BEEM we do not get any further information about the structural and chemical nature of these atomic-size defects, their mere observation is nevertheless an important result. In recent years evidence has been growing that even the presumably most perfect heterointerfaces are not perfectly ordered, but contain point defects on a nanometer scale.²⁰ BEEM allows one to locate such point

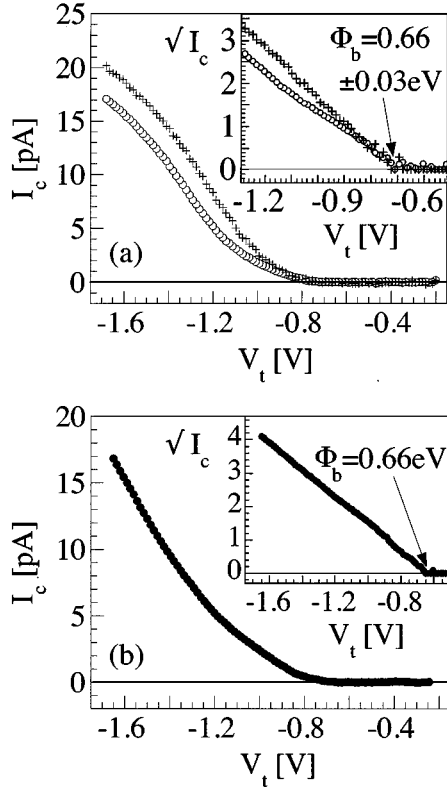


FIG. 2. (a) BEES spectra right on top of a dislocation (crosses), like the one in Fig. 1(a), and in the neighboring dislocation free region (open circles). The spectra were taken on a 35-Å $\text{CoSi}_2/n\text{-Si}(111)$ film. The subtle spectral features near the threshold are due to quantum interference effects in CoSi_2 (Ref. 22). In the inset is shown the square root of the BEES current. At the dislocation the BEES current sets in at the same value as in the adjacent dislocation free region. (b) BEES spectrum taken in the apparently point defect and dislocation free region (B) in Fig. 1(b). In the inset the square root of the BEES current is displayed ($I_t = 5$ nA). Even in this region no evidence of a delayed BEES onset is seen.

defects, and more importantly, to investigate their effect on the carrier transmission across the interface.

The above results prove that the probability α for the electrons to be scattered at the interface is significantly enhanced locally at interfacial dislocations. However, this does not necessarily imply that α is strictly zero *in dislocation free regions*. Indeed, during the course of our experiments several pieces of evidence have been found that suggest that, even in dislocation free regions, the scattering probability α is finite.

(a) As has been shown in Fig. 1, in the dislocation free regions point defects with a density on the order of $10^{12}\text{--}10^{13}\text{ cm}^{-2}$ exist, at which the carriers are scattered.

(b) We observe a contribution to the BEES current from states in two-dimensional hole subbands confined in CoSi_2 . Those states are formed by quantum interference,²¹ and lie close to the center of the IBZ, where $T(E, k_{\parallel}) = 0$, i.e., where the electrons are confined in CoSi_2 . Therefore, they can only contribute to the BEEM current, if k_{\parallel} is not strictly conserved.²²

(c) The magnitudes of the BEEM current on $\text{CoSi}_2/n\text{-Si}(100)$ and $n\text{-Si}(111)$ are comparable.¹⁴

(d) The experimental BEES spectra do not exhibit a delayed BEES onset, as predicted by theory. A theoretical calculation of the ITP $T(E, k_{\parallel})$ (Ref. 10) shows that for energies up to 0.85 eV above $E_F^{\text{CoSi}_2}$ there is no overlap between the projected phase space of Si and CoSi_2 in the (111) IBZ. As a consequence, the BEES onset should be delayed by ≈ 0.2 eV from the value of the Schottky barrier. However, we observe an onset right at the Schottky barrier, at $V_t = 0.66$ V.²³ Provided that the accuracy of the theoretical calculation is sufficient to allow for a direct comparison with the experiment,²⁴ this would be an unambiguous proof for a non-zero α because below $V_t \approx 0.85$ eV electrons can only cross the interface by a k_{\parallel} -violating process. It is important to note that *even in dislocation and point defect free regions* we do not see any evidence of a delayed BEES onset, nor of a second threshold around $V_t \approx 0.85$ eV. This is shown in Fig. 2(b), where the spectrum taken in the point defect free region (B) in Fig. 1(b) is displayed.

From the ensemble of these results we regard it as likely that a certain probability for scattering exists *everywhere* at the epitaxial CoSi_2/Si interface. At present we feel unable to give a reliable quantitative estimate of α . However, it should be emphasized that α cannot be close to 1, as it would be at a completely disordered interface, because this would contradict the significant enhancement of the scattering probability at individual interfacial defects and the formation of quantum interference states in CoSi_2 .²¹

What might be the additional scattering mechanism that is responsible for a nonzero scattering probability *everywhere* at the epitaxial CoSi_2/Si interface? The absence of a delayed BEES onset in regions such as (B) in Fig. 1(b) renders it improbable that the scattering mechanism is related to the presence of the localized point defects (A), which are resolved in BEEM images with a density on the order of $10^{12}\text{--}10^{13}\text{ cm}^{-2}$. In view of the BEEM attenuation length on the order of 100 Å and the small interfacial area illuminated by the electron beam it appears rather improbable that the nearest localized interfacial defects, which are more than 50 Å away, strongly scatter the electrons, even if multiple passes through the metal are taken into account. We conclude that the interface scattering mechanism responsible for the absence of a delayed onset in the experimental BEES spectra, even in apparently perfectly ordered regions, must be an inherent one, such as electron phonon scattering at the interface, rather than scattering at localized interfacial defects. The possibility of electron-phonon scattering might be tested in the future by temperature-dependent experiments down to 4 K.

IV. SCHOTTKY BARRIER FLUCTUATIONS AT THE $\text{CoSi}_2/\text{Si}(100)$ INTERFACE ON A NANOMETER SCALE

We now turn to the $\text{CoSi}_2/\text{Si}(100)$ interface. Because of the different atomic interface structure other types of dislocations occur at this interface. It will be shown that their effect on the interface transmission is fundamentally different from the simple scattering mechanism observed at the $\text{CoSi}_2/\text{Si}(111)$ interface. In this section we discuss only dislocations rather than point defects, because at the (100) interface we have not been able to resolve point defects. This

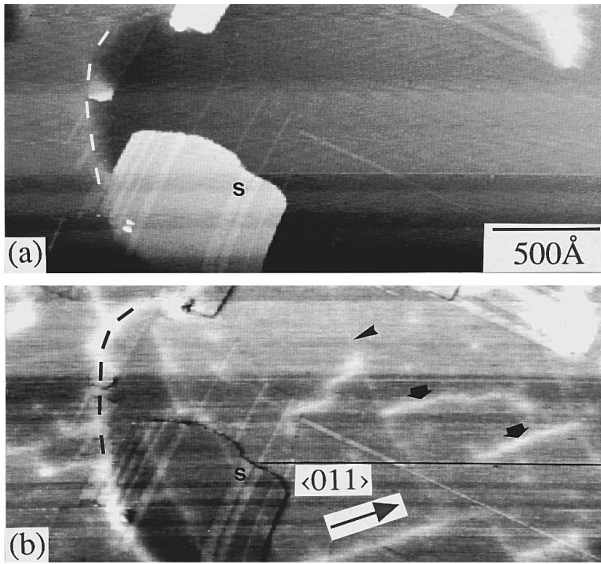


FIG. 3. STM topograph (a) and BEEM image (b) on a 30-Å $\text{CoSi}_2/3000 \text{ \AA } i\text{-Si}/n^+\text{-Si}(100)$ film. The dashed lines indicate a $\mathbf{b}=(a/4)\langle 111 \rangle$ interfacial dislocation; the broad arrows point to other linear defects at the interface. At those interfacial defects the BEEM current is enhanced by typically 20% due to a lowering of the Schottky barrier on a nanometer scale ($V_t = -2 \text{ V}$, $I_t = 3 \text{ nA}$).

does not mean that point defects do not exist at this interface. As discussed below, their observation may be prevented by the complicated (100) surface reconstructions and surface scattering.

The STM and BEEM images in Fig. 3 show a 30-Å $\text{CoSi}_2/n\text{-Si}(100)$ film. Two different types of interfacial defects are observed in this image: Near the left edge runs a $\mathbf{b}=(a/4)\langle 111 \rangle$ misfit dislocation. Dislocations of this kind occur at monolayer steps on the Si substrate with a height of $a/4 = 1.35 \text{ \AA}$ (see Fig. 4), because the minimum step height in the silicide is $a/2$ rather than $a/4$. The silicide covers such steps on the substrate smoothly, i.e., without an interfacial step in the silicide. Since the silicide thickness on both sides of the interfacial step is the same, this gives rise to a smooth topographic contrast of 1.35 \AA in the STM topography, which indicates the position of the $\mathbf{b}=(a/4)\langle 111 \rangle$ dislocation at the interface. Such a topographic contrast is observed at

the dashed line in Fig. 3(a). These dislocations give rise to an increase of the BEEM current. In addition, the BEEM current is also enhanced in the linear regions indicated by the two broad arrows. These bright lines are along the $\langle 011 \rangle$ direction and have a typical length of 500–1000 Å. They end abruptly somewhere at the interface; i.e., they do not form a continuous network. There might, however, be weaker lines, which are barely resolved in Fig. 3(b) (thin arrow), but appear to connect the bright lines. This contrast is clearly due to some subsurface linear defect, because on the surface there is neither an atomic-scale discontinuity nor a long-range surface distortion. The surface in Fig. 3 is homogeneously $3\sqrt{2} \times \sqrt{2}R45^\circ$ ($3\sqrt{2}$ in short) reconstructed. Only on some small stripes, one of them being labeled *S* in Fig. 3, we have resolved a $\sqrt{2} \times \sqrt{2}R45^\circ$ ($\sqrt{2}$) surface reconstruction. These $\sqrt{2}$ stripes, oriented along the $\langle 100 \rangle$ direction, appear slightly brighter in the STM and BEEM images. This surface effect is due to a dependence of the magnitude of the BEEM current on the atomic surface structure and has been investigated elsewhere.²⁶ In the following the unusual interfacial defects will be denoted as “linear defects,” distinguishing them from the $\mathbf{b}=(a/4)\langle 111 \rangle$ dislocations.

The contrast in the BEEM image at the interfacial defects cannot be due to scattering as on $\text{CoSi}_2/\text{Si}(111)$. Two of the six CBM project onto the zone center of the $\text{CoSi}_2/n\text{-Si}(100)$ IBZ. For the same reason as on $\text{CoSi}_2/p\text{-Si}(111)$, scattering should decrease rather than increase the BEEM current. Therefore, a different contrast mechanism must be dominant in this case. Figure 5 displays BEES spectra measured right on top of a $\mathbf{b}=(a/4)\langle 111 \rangle$ dislocation and in the neighboring dislocation free region. From a fit to a quadratic power law, i.e., $I_c = R(V_t - \Phi_b)^2$, (Ref. 3) we find that the Schottky barrier Φ_b at the dislocation is lower by 0.04–0.08 eV than the value of 0.75 eV in the dislocation free region. We observe some variation of Φ_b along the dislocation line, whose origin is not understood at present. However, the shift of the BEES onset (see inset) is statistically significant. The *R* value on top of the dislocation is larger by 50–80% than in the neighboring region.

A similar lowering of the Schottky barrier is observed at the linear defects [see Fig. 6(a)]. It is even more pronounced and amounts to 0.1 eV, whereas the scale factor *R* is about the same on top of the linear defect and in the defect free

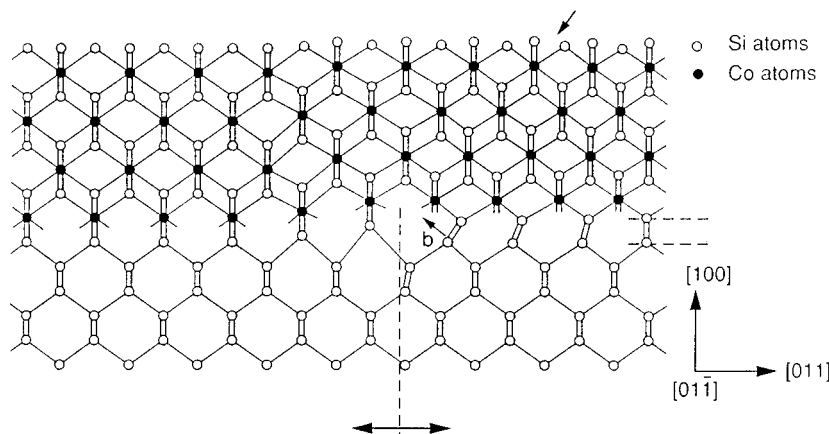


FIG. 4. Schematic diagram of the atomic structure at the $\text{CoSi}_2/\text{Si}(100)$ interface. A monolayer interfacial step with a height of $a/4 = 1.35 \text{ \AA}$ is associated with a $\mathbf{b}=(a/4)\langle 111 \rangle$ dislocation. On both sides of the step the interface is unreconstructed. The same dislocation may also occur at the 2×1 reconstructed interface. (From Ref. 25.)

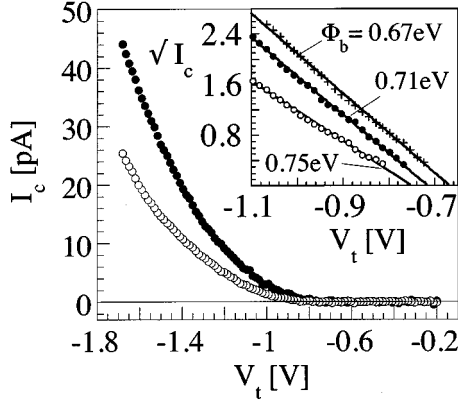


FIG. 5. BEES spectra taken on top of a $\mathbf{b}=(a/4)\langle 111 \rangle$ dislocation (filled circles) and in the neighboring dislocation free region (open circles) (see Fig. 3). In the inset the square root of the BEES current near the threshold is shown. The spectrum drawn by crosses belongs to a different location on top of the dislocation ($I_t=3$ nA). On top of the $\mathbf{b}=(a/4)\langle 111 \rangle$ dislocation the Schottky barrier is lowered.

region. This can clearly be seen in the inset of Fig. 6(a), where the square root of the spectra is shown. This is clear proof that the BEEM contrast observed at both the $\mathbf{b}=(a/4)\langle 111 \rangle$ dislocations and the linear defects is due to a lowering of the Schottky barrier, in contrast to the one observed at misfit dislocations at the $\text{CoSi}_2/\text{Si}(111)$ interface [compare Fig. 2(a)].

The behavior of the R value at the dislocation is difficult to interpret. From the results presented in Sec. III one might expect R to be decreased at the dislocation due to scattering effects. However, it should be kept in mind that the parameter R does not only reflect scattering effects. R also depends in a complicated way on the value of the local Schottky barrier height, i.e., on the band lineup, because Φ_b determines which silicide states couple to the Si CBM in the IBZ.¹⁰ Furthermore, in the case of the $\mathbf{b}=(a/4)\langle 111 \rangle$ dislocations surface effects also have to be considered. Right at the smooth surface step associated with the dislocation we usually observe a small stripe with the $\sqrt{2}$ surface structure, whereas the rest of the surface is $3\sqrt{2}$ reconstructed. This change of surface structure is possibly induced by the surface strain around the smooth surface step. The $\sqrt{2}$ surface does not affect the BEES onset, of course, but it gives rise to a larger magnitude of the BEEM current, i.e., a larger R value.²⁶ This can be clearly seen on the $\sqrt{2}$ stripe S , which exhibits a higher BEEM current than the surrounding $3\sqrt{2}$ regions on that terrace.²⁷ The absence of a decreased R value on top of the dislocations suggests that scattering effects might be masked by such band lineup and surface effects.

To investigate the spatial variation of the potential profile in more detail we have taken BEES spectra such as those in Fig. 6(a) as a function of the distance perpendicular to the linear defect. By fitting the individual spectra to the above quadratic power law we obtain a profile of the BEES onset Φ_b and the scale factor R across a linear defect [see Fig. 6(b)]. To quantify the lateral width of the region exhibiting a lower Schottky barrier height, the Φ_b profile has been fit to a Lorentzian (solid line). The fit yields a FWHM of 40 ± 5 Å. Similar values are obtained for the $\mathbf{b}=(a/4)\langle 111 \rangle$ disloca-

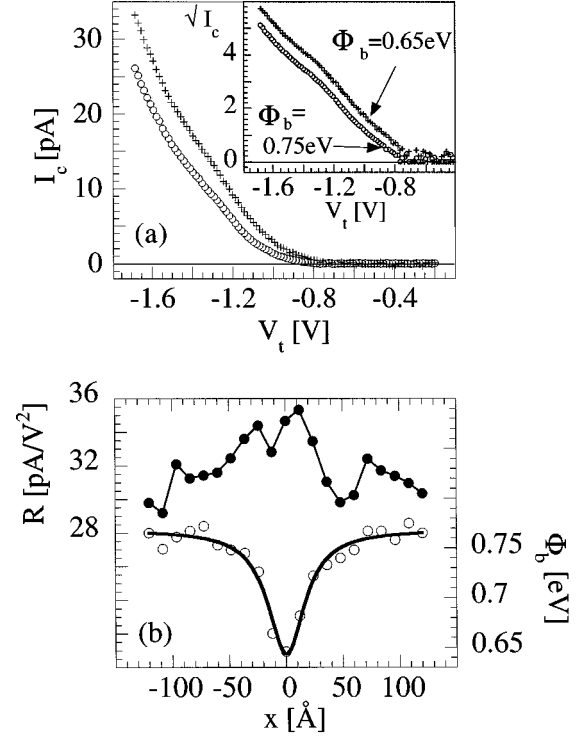


FIG. 6. (a) BEES spectra measured on top of the linear defects (crosses) and in the neighboring defect free region (open circles). In the inset the square root of the BEES current is shown ($I_t=3$ nA). It can be seen clearly that also on top of the linear defects the Schottky barrier is lowered, in contrast to $\text{CoSi}_2/\text{Si}(111)$ [compare Fig. 2(a)]. (b) Profile of the BEES onset Φ_b and the scale factor R across a linear defect. The solid line is a fit of the potential profile to a Lorentzian yielding a FWHM of 40 ± 5 Å.

tions. The Φ_b profile is a map of the potential barrier *on a truly nanometer scale*.

The observed lowering $\delta\Phi_b$ of the Schottky barrier is caused by a lowering of the electrostatic potential at the interface by an amount Δ . The quantity Δ is more fundamental than $\delta\Phi_b$, because the latter is affected by the screening of the true potential variation at the interface in the semiconductor (“pinch-off effect”),²⁸ i.e., is strongly dependent on the doping characteristics of the semiconductor. Far away from the defect the potential energy in the undoped Si buffer layer decreases linearly from its value $\Phi_b^0 = V_{bb} + V_n = 0.75$ eV at the interface ($z=0$) to V_n at the interface between the buffer and the degenerately doped substrate ($z=W=3000$ Å). (V_{bb} is the band bending in the buffer.) Note that in a homogeneously doped semiconductor the variation would be quadratic rather than linear. Following Tung²⁹ let us assume that *at the interface* the potential is lowered by an amount Δ from its value $\Phi_b^0 = 0.75$ eV far away from the defect in an infinitely long stripe of width L_0 ($-L_0/2 < x < L_0/2$). Neglecting the effect of the image force the potential in the semiconductor is given by

$$V(x, z) = V_{bb} \left(1 - \frac{z}{W} \right) + V_n - \frac{\Delta}{\pi} \left(\tan^{-1} \frac{|x| + L_0/2}{z} - \tan^{-1} \frac{|x| - L_0/2}{z} \right). \quad (1)$$

Within this model Δ can be estimated from the value $\delta\Phi_b$ at the center of the defect ($x=0$):

$$\Delta \approx \frac{\pi W \delta\Phi_b^2}{4 V_{bb} L_0}. \quad (2)$$

An upper limit for L_0 can be estimated from the FWHM of the potential profiles such as the one in Fig. 6(b), i.e., $L_0^{\min} \approx 40 \text{ \AA}$. L_0 might be smaller than this value because the FWHM might be affected by the spatial extent of the electron beam at the interface.³⁰ If we assume an average value of $\delta\Phi_b = 0.06 \text{ eV}$ for the $\mathbf{b}=(a/4)\langle 111 \rangle$ dislocations we obtain a lower limit for Δ : $\Delta^{\min} \approx 0.3 \text{ eV}$; i.e., Δ must be significantly larger than $\delta\Phi_b$ (pinch-off regime). For the 0.1-eV lowering at the linear defects we obtain values for Δ that are close to or even larger than Φ_b^0 . However, for such large lowerings on a nanometer scale, resulting in large electric fields, a classical treatment may no longer be appropriate.

The observation by BEEM of Schottky barrier fluctuations on a nanometer scale has been reported already for the Au/Si and Au/GaAs system.^{31,32} However, in these studies the nature of the corresponding interfacial defects could not be identified. They are most probably related to chemical intermixing at the interface. Here, at least in the case of the $\mathbf{b}=(a/4)\langle 111 \rangle$ dislocations, we can attribute the lowering of the potential barrier to a known structural defect at the interface, for which even a structure model (see Fig. 4) has been proposed.²⁵ This will be useful for a theoretical understanding of the relationship between the Schottky barrier fluctuations and the atomic interface structure around the dislocation.

In the case of the linear defects, however, the structural nature is not known at present. It appears that they cannot be identified with any of the dislocations that have been observed in a thorough transmission electron microscopy (TEM) study of the CoSi₂/Si(100) interface.²⁵ The BEES spectra taken to the left and to the right of a linear defect are identical up to voltages of at least -6 V . This renders it improbable that the linear defect is due to a phase boundary between two different interface structures. From the lack of a BEEM contrast at high voltages between the two adjacent regions it can be excluded that the linear defects are associated with an interfacial step. Since there is no topographic contrast at the surface across the defect, an interfacial step would imply a change of the metal film thickness, and show up as an attenuation-related BEEM contrast at high voltages.¹⁴

Two different CoSi₂/Si(100) interface structures have been identified by TEM: a 2×1 reconstructed and an unreconstructed interface.²⁵ In our films TEM investigations have shown the interface to be predominantly 2×1 reconstructed.

It is conceivable that the linear defects are formed by a thin unreconstructed stripe embedded in a predominantly 2×1 reconstructed interface region. Another possibility would be small, nanometer-size troughs formed by (111) microfacets, which have been observed at the related NiSi₂/Si(100) interface.³³ However, up to now neither plan-view nor cross-sectional TEM investigations on the sample shown in Fig. 3 have been successful in identifying linear defects compatible with those observed by BEEM.

V. CONCLUSIONS

In this work we have investigated the contrast mechanisms by which individual interfacial defects at the epitaxial CoSi₂/Si interface can be resolved by BEEM. At the CoSi₂/Si(111) interface the probability for the carriers to be scattered at the interface is significantly enhanced by individual interfacial dislocations and point defects. This establishes BEEM as one of few experimental techniques by which point defects at a buried interface can be detected, and, more importantly, by which their effect on the carrier transmission across the interface can be investigated. Even in apparently perfectly ordered interfacial regions we have found evidence for a finite scattering probability at the interface. This suggests the presence of an additional inherent scattering mechanism such as electron-phonon scattering at the interface. At the CoSi₂/Si(111) interface the Schottky barrier is homogeneous. However, at the CoSi₂/Si(100) interface partial misfit dislocations and certain linear defects, whose structure has not been identified yet, give rise to a significant lowering of the Schottky barrier on a nanometer scale. These BEEM results together with the information from TEM about the atomic structure at the interface might be useful for theoretically understanding the relationship between interfacial defects and the local band lineup at the interface, as well as the effect of the presence of such defects on the average Schottky barrier height extracted from the transport characteristics of a macroscopic diode. The reason that at the (100) interface certain dislocations lower the Schottky barrier whereas at the (111) interface they do not, must be related to the specific atomic structure at the interface.

ACKNOWLEDGMENTS

It is a pleasure to thank N. Onda for the electrical characterization of the diodes, E. Müller for the TEM investigations, and U. Kafader for assistance with the sample preparation. Financial support from the Swiss National Science Foundation (NFP 24) and the Swiss Research Foundation is gratefully acknowledged.

¹M. Ono, M. Saito, T. Yoshimoti, C. Fiegna, T. Ohguro, H. Sasaki Momose, and H. Iwai, *J. Vac. Sci. Technol. B* **13**, 1740 (1995).

²W. J. Kaiser and L. D. Bell, *Phys. Rev. Lett.* **60**, 1406 (1988); L. D. Bell and W. J. Kaiser, *ibid.* **61**, 2368 (1988).

³For a recent review, see, e.g., M. Prietsch, *Phys. Rep.* **253**, 163 (1995).

⁴L. D. Bell, S. J. Manion, M. H. Hecht, W. J. Kaiser, R. W. Fathauer, and A. M. Milliken, *Phys. Rev. B* **48**, 5712 (1993).

⁵T.-H. Shen, M. Elliott, A. E. Fowell, A. Cafolla, B. E. Richardson, D. Westwood, and R. H. Williams, *J. Vac. Sci. Technol. B* **9**, 2219 (1991).

⁶T. Sajoto, J. J. O'Shea, S. Bhargava, D. Leonard, M. A. Chin, and

- V. Narayanamurti, Phys. Rev. Lett. **74**, 3427 (1995).
- ⁷M. T. Cuberes, A. Bauer, H. J. Wen, M. Prietsch, and G. Kaindl, Appl. Phys. Lett. **64**, 2300 (1994).
- ⁸R. Ludeke, A. Bauer, and E. Cartier, Appl. Phys. Lett. **66**, 730 (1995).
- ⁹H. Siringhaus, E. Y. Lee, and H. von Känel, Phys. Rev. Lett. **73**, 577 (1994).
- ¹⁰M. D. Stiles and D. R. Hamann, J. Vac. Sci. Technol. B **9**, 2394 (1991).
- ¹¹W. E. Spicer, Z. Lilienthal-Weber, E. R. Weber, N. Newman, T. Kendelewicz, R. Cao, C. McCants, K. Miyano, P. H. Mahowald, and I. Lindau, J. Vac. Sci. Technol. B **6**, 1245 (1988).
- ¹²For a review, see, e.g., W. Mönch, Rep. Prog. Phys. **53**, 221 (1990).
- ¹³H. von Känel, Mat. Sci. Rep. **8**, 193 (1992).
- ¹⁴E. Y. Lee, H. Siringhaus, U. Kafader, and H. von Känel, Phys. Rev. B **52**, 1816 (1995).
- ¹⁵H. Siringhaus, E. Y. Lee, and H. von Känel, J. Vac. Sci. Technol. B **12**, 2629 (1994); H. Siringhaus, Ph.D. thesis, ETH Zürich, 1995.
- ¹⁶H. von Känel, E. Y. Lee, and H. Siringhaus, Thin Solid Films **267**, 89 (1995).
- ¹⁷J. C. Hensel, R. T. Tung, J. M. Poate, and F. C. Unterwald, Phys. Rev. Lett. **54**, 1840 (1985).
- ¹⁸H. von Känel and G. Fishman, Phys. Rev. B **45**, 3929 (1992).
- ¹⁹H. Siringhaus, T. Meyer, E. Y. Lee, and H. von Känel, Surf. Sci. **357-358**, 386 (1996).
- ²⁰M. B. Johnson, U. Maier, H. P. Meier, and H. W. M. Salemink, Appl. Phys. Lett. **63**, 1273 (1993).
- ²¹E. Y. Lee, H. Siringhaus, and H. von Känel, Phys. Rev. B **50**, 5807 (1994).
- ²²H. Siringhaus, E. Y. Lee, and H. von Känel, Surf. Sci. **331-333**, 1277 (1995).
- ²³A delayed BEES onset had been reported in earlier, *ex situ* experiments [see W. J. Kaiser, M. H. Hecht, R. W. Fathauer, L. D. Bell, E. Y. Lee, and L. C. Davis, Phys. Rev. B **44**, 6546 (1991)]. This result could not be confirmed in our experiments nor in the ones by Schulz *et al.* (see H. Schulz, Ph.D. thesis, Universität Erlangen, 1994).
- ²⁴It should be pointed out that the prediction of a delayed onset due to the lack of common phase space at the Si CBM is not too sensitive to the accuracy of the band structure computation. To obtain some overlap right at the Si CBM the lowest unoccupied silicide state with the same k_{\parallel} as the Si CBM would have to be lower by ≈ 0.6 eV than the value predicted by the band structure calculation.
- ²⁵C. W. T. Bulle Lieuwma, A. F. de Jong, and D. E. W. Vandenhoudt, Philos. Mag. A **64**, 255 (1991).
- ²⁶H. Siringhaus, E. Y. Lee, and H. von Känel, Phys. Rev. Lett. **74**, 3999 (1995).
- ²⁷It should be mentioned that the average BEEM current on the terrace, on which *S* is located, is slightly smaller than on the other regions. However, this is related to the attenuation of the BEEM current in the metal film, which is thicker by 2.7 Å on the terrace than on the other regions.
- ²⁸J. L. Freeouf, T. N. Jackson, S. E. Laux, and J. M. Woodall, J. Vac. Sci. Technol. **21**, 570 (1982).
- ²⁹R. T. Tung, Phys. Rev. B **45**, 13 509 (1992).
- ³⁰On $\text{CoSi}_2/\text{Si}(100)$ we have not been able to resolve interfacial point defects such as those on $\text{Si}(111)$, whose apparent size could have been used for an estimate of the beam width at this interface. This is presumably due to the complicated surface reconstructions ($\sqrt{2}/3\sqrt{2}$) giving rise to strong surface induced contrast variations and surface scattering (see Ref. 19).
- ³¹H. Palm, M. Arbres, and M. Schulz, Phys. Rev. Lett. **71**, 2224 (1993).
- ³²A. A. Talin, R. S. Williams, B. A. Morgan, K. M. Ring, and K. L. Kavanagh, Phys. Rev. B **49**, 16 474 (1994).
- ³³D. Cherns, C. J. D. Hetherington, and C. J. Humphreys, Philos. Mag. A **49**, 165 (1984).